Supplementary Materials for

Self-assembling RuO_2 nanogranulates with few carbon layers as an interconnected nanoporous structure for lithium-oxygen batteries

Wei-Hong Lai, Zhi Zheng, Wanlin Wang, Lei Wang, Yao-Jie Lei, Yun-Xiao Wang, Jia-Zhao Wang, Hua-Kun Liu, Shu-Lei Chou, Shi-Xue Dou

Methods

Synthesis of nanoporous RuO_2@C

One gram of soluble starch was dissolved in 10.0 mL distilled water with stirring. Then, it was mixed with a 10 mL aqueous solution of Ruthenium chloride (0.1 M) to form a uniform suspension. The mixture was then placed in an oil bath preheated to 80 °C and maintained for 20 min under vigorous stirring until a pink gel was obtained. The gelatinized paste was kept at 80 °C for an additional 10 min without stirring to age. After cooling to room temperature, it was then freeze-dried for 72 h to obtain the Ru^{3+}/starch precursor. Then, the precursor was calcined at a temperature of 500 °C with a heating rate of 5 °C min^{-1} to obtain the hierarchically 3D nanoporous RuO_2@C.

Characterization. The morphologies of the samples were investigated by field-emission scanning electron microscopy (FESEM; JEOL JSM-7500FA) and transmission electron microscopy (TEM, JEOL 2011, 200 kV). The high-angle annular dark-field scanning TEM (HAADF-STEM) images and the scanning TEM energy dispersive X-ray spectroscopy (STEM-EDS) data were acquired on the transmission electron microscopy system (TEM, JEOL ARM-200F, 200 kV). The XRD patterns were collected by powder X-ray diffraction (XRD; GBC MMA diffractometer) with Cu Kα radiation at a scan rate of 4 ° min^{-1}. The valence status was determined by XPS (PHOIBOS 100 Analyser from SPECS, Berlin, Germany; Al Kα X-rays). Synchrotron powder diffraction data were collected at the Australian Synchrotron beamline with a wavelength (λ) of 0.0.7749 Å (National Institute of Standards and Technology (NIST) LaB6 660b).

Electrochemical Measurements. Before the glassy carbon electrode (GCE) was used, it was consecutively polished with 1.0 and 0.05 μm alumina powder, rinsed with deionized water, and sonicated first in ethanol and then in water. Electrochemical experiments of OER were carried out in 0.1 M KOH by using a computer-controlled potentiostat (Princeton 2273 and 616, Princeton Applied Research) in a conventional three-electrode cell at room temperature. Typically, working electrodes were prepared by mixing the catalyst with deionized water + isopropanol + 5% Nafion® (v/v/v = 4/1/0.05). A Pt wire was used as the counter electrode and Ag/AgCl (KCl, 3M) was used as the reference electrode, with all potentials referred to reversible hydrogen electrode (RHE). Thus, the potential with respect to RHE can be calculated as follows: E(RHE) = E(Ag/AgCl) + 0.059 × pH + 0.210. Before testing, flowing N_2 was bubbled through the electrolyte in the cell to achieve an N_2 -saturated solution.

Li-O_2 Battery Measurements. The electrochemical performances of lithium oxygen batteries were investigated using 2032 coin-type cells with air holes on the cathode side. For the

preparation of the H-PtCo/Pt@zNPC cathode electrode, 70 wt. % catalyst, 20 wt. % Super P, and 10 wt. % poly(1,1,2,2-tetrafluoroethylene) (PTFE) were mixed in an isopropanol solution. The resulting homogeneous slurry was coated on carbon paper. After that, the electrodes were dried at 120 ºC in a vacuum oven for 12 h. All the Li-O_2 batteries were assembled in an Ar-filled glove box (Mbraun, Unilab, Germany) with water and oxygen contents below 0.1 ppm. They contained lithium metal foil as the counter electrode and a glass fiber separator (Whatman GF/D). One electrolyte consisted of 1 M $LiCF_3SO_3$ in tetraethylene glycol dimethyl ether (TEGDME). All the assembled coin cells were stored in an O_2 purged chamber which was connected to a LAND CT 2001 instrument. The galvanostatic discharge-charge tests were then conducted on the battery testing system. All the capacities were calculated based on the mass of active materials in the cathode.

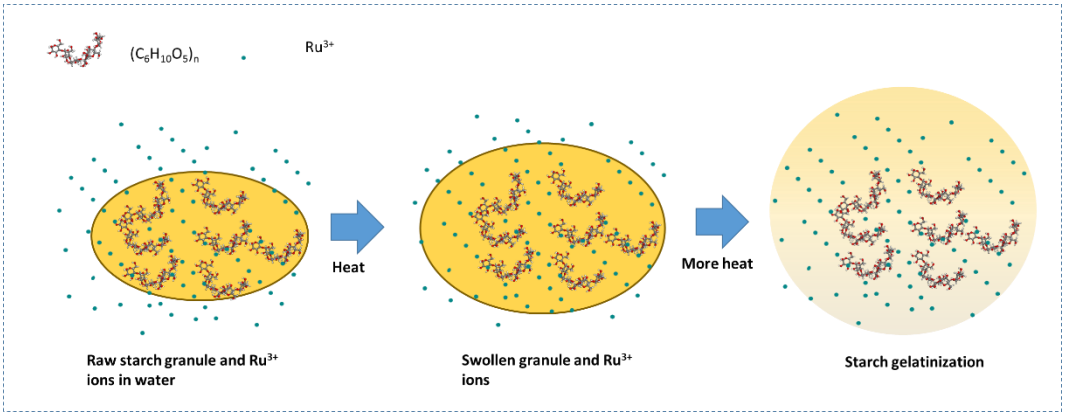

Figure S1. The schematic illustration of starch gelatinization with Ru^{3+} ions.

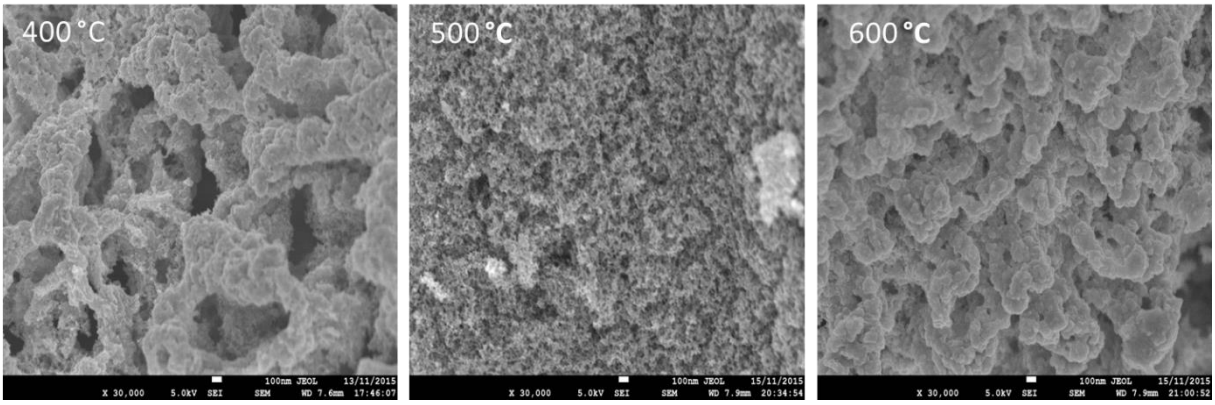

Figure S2. The SEM images of RuO_2@C after calcination at different temperatures.

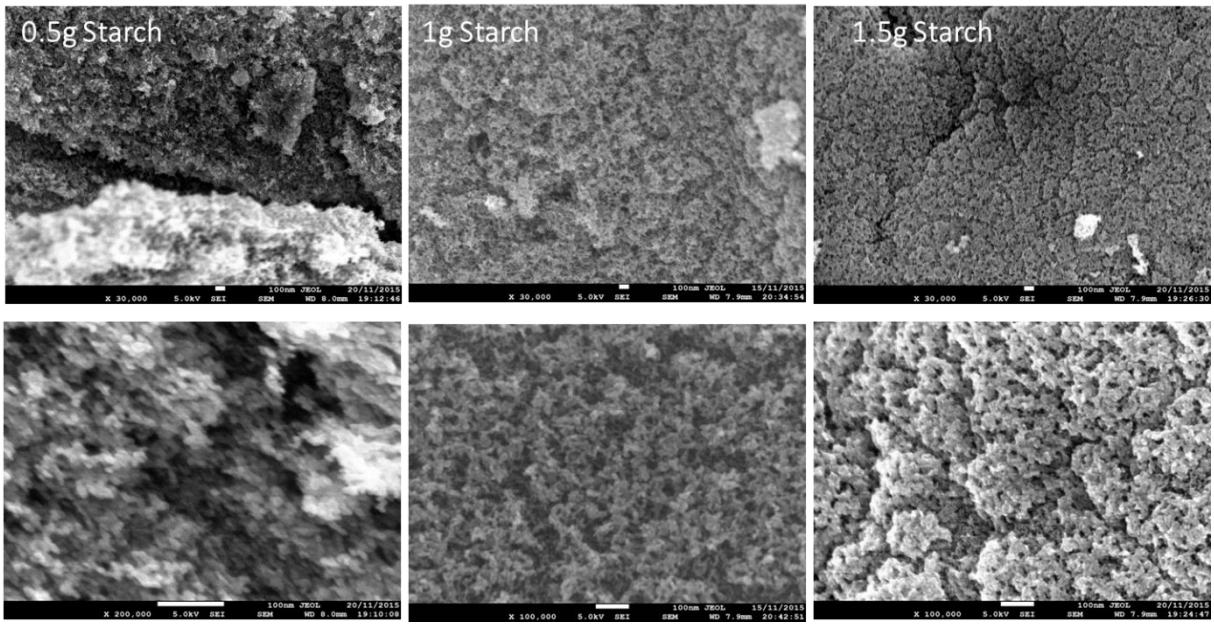

Figure S3. The SEM images of RuO_2@C with different amounts of starch.

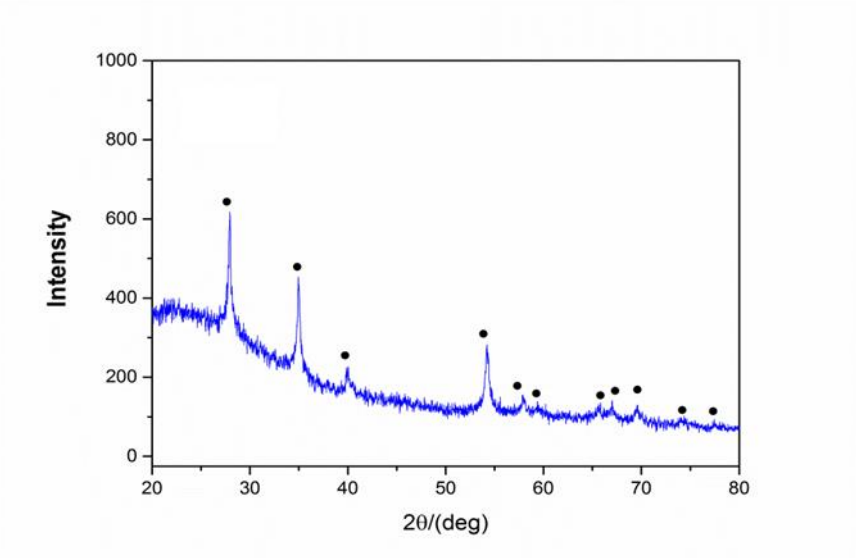

Figure S4. The XRD pattern of RuO_2@C.

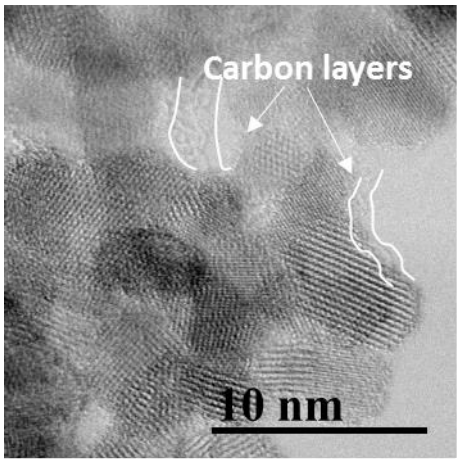

Figure S5. The HRTEM image of RuO_2@C.

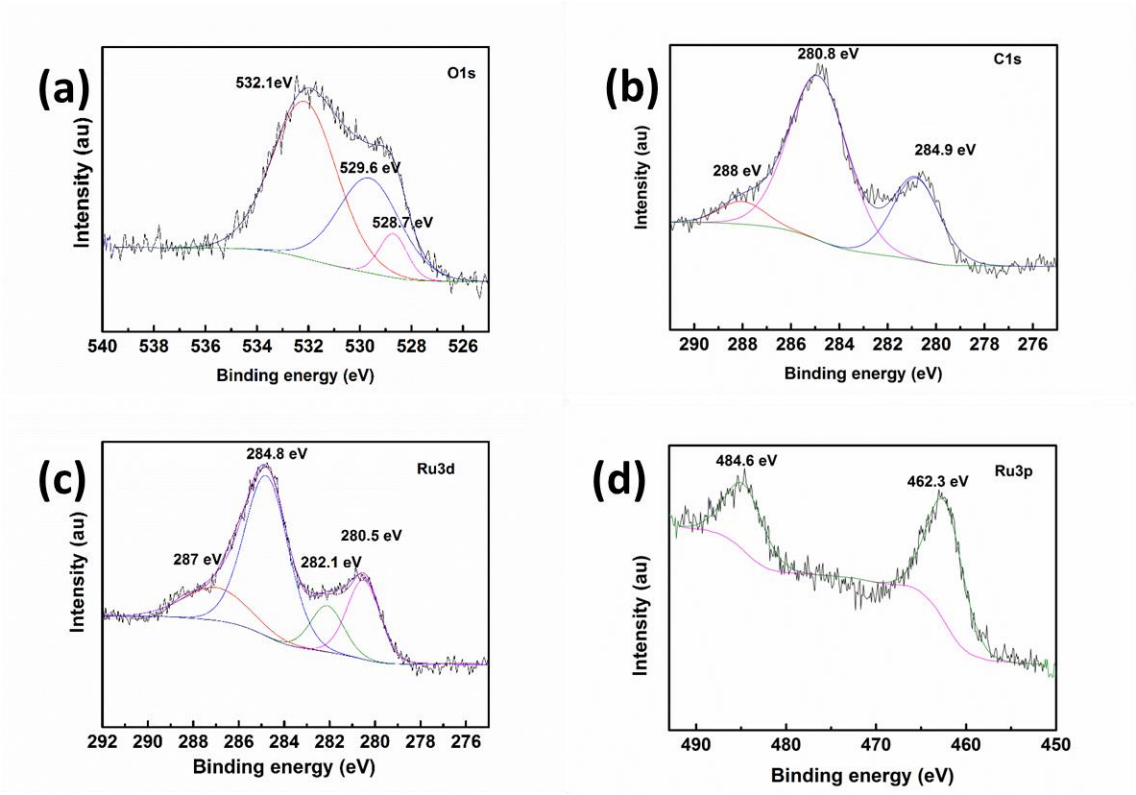

Figure S6. High-resolution XPS spectra of (a) O 1s, (b) C 1s, (c) Ru 3d, and (d) Ru 3p.

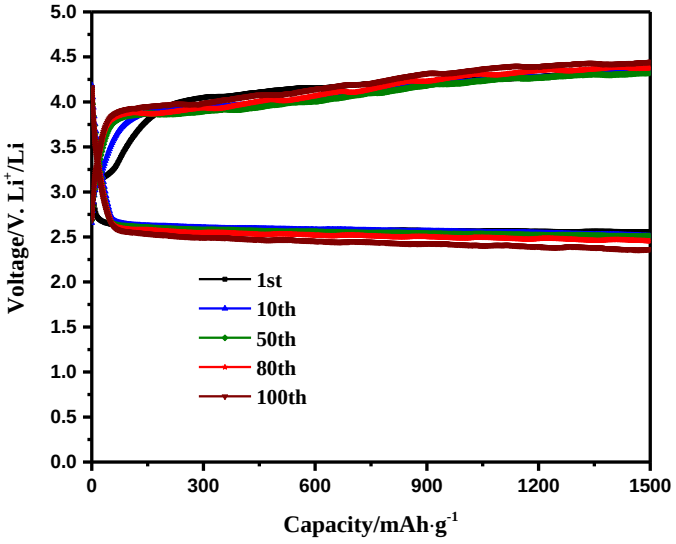

Figure S7. The charge/discharge curves at various cycles.

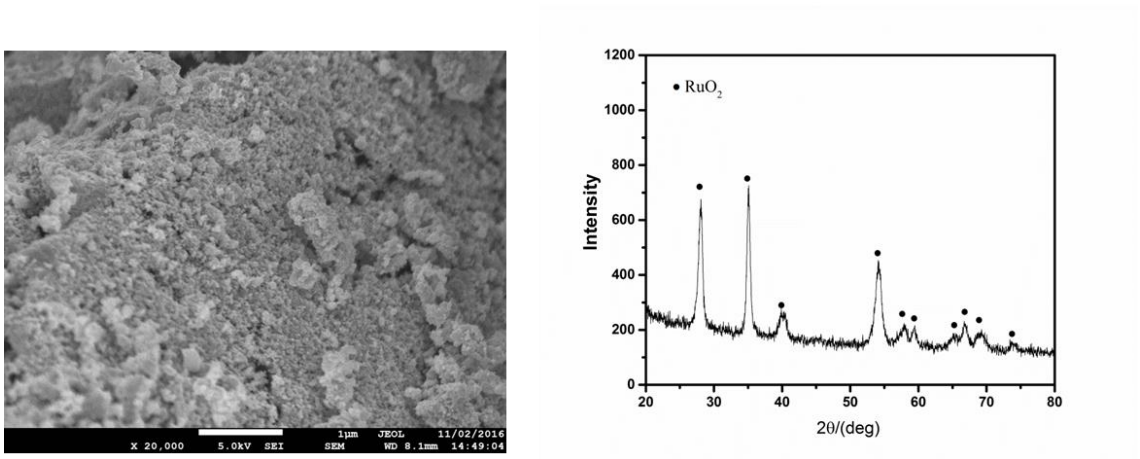

Figure S8. The SEM image (left) and XRD pattern (right) of pure RuO_2.

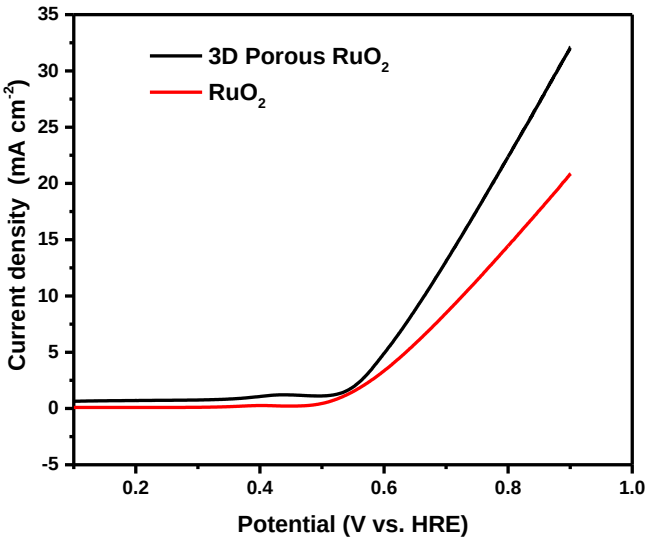

Figure S9. The comparative OER polarization curves of commercial RuO_2 and 3D nanoporous RuO_2@C.

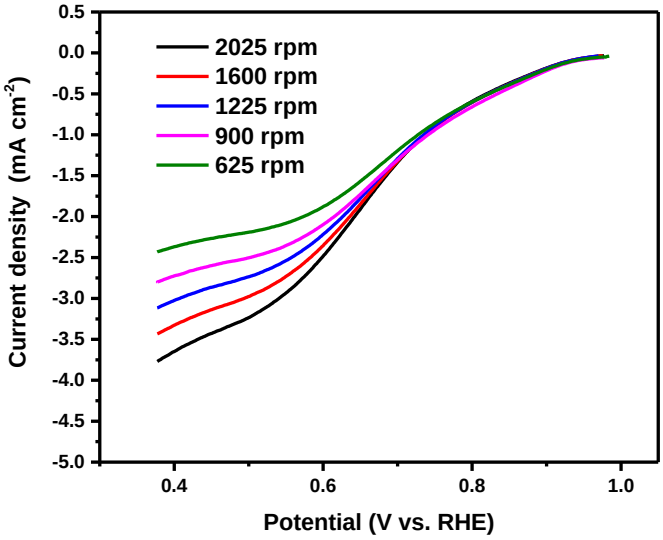

Figure S10. The ORR polarization curves of 3D nanoporous RuO_2@C with different rotating speed.

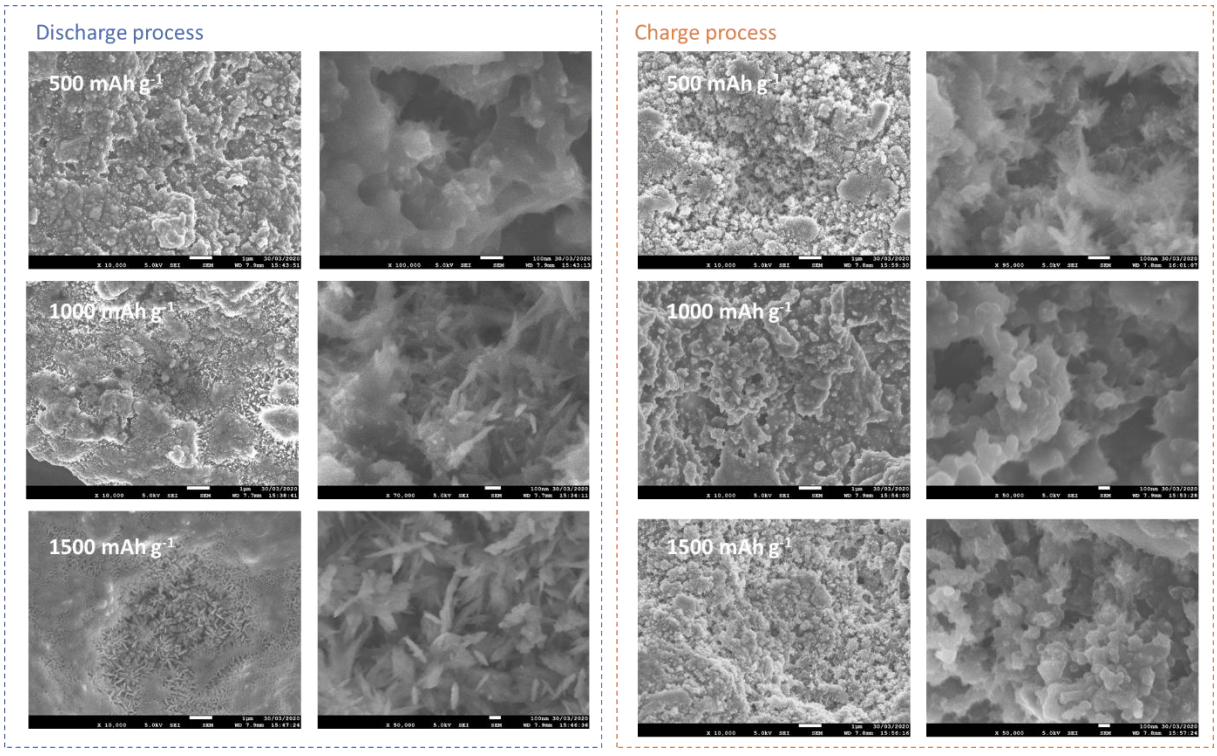

Figure S11. The SEM images of porous RuO_2@C after discharge/charge with a capacity limitation of 500, 1000, and 1500 mAh g^{-1}.